

Stochastic Backlog and Delay Bounds of Generic Rate-based AIMD Congestion Control Scheme in Cognitive Radio Sensor Networks

Vahid Esmaeelzadeh^a, Reza Berangi^a, Elahe S. Hosseini^a, Ozgur B. Akan^b

^a*Wireless Networks Laboratory (WNL), Department of Computer Engineering,
Iran University of Science and Technology, Tehran, Iran.*

^b*Next-generation and Wireless Communications Laboratory (NWCL),
Department of Electrical and Electronics Engineering, Koc University, Istanbul, Turkey*

Abstract

Performance guarantees for congestion control schemes in cognitive radio sensor networks (CRSNs) can be helpful in order to satisfy the quality of service (QoS) in different applications. Because of the high dynamicity of available bandwidth and network resources in CRSNs, it is more effective to use the stochastic guarantees. In this paper, the stochastic backlog and delay bounds of generic rate-based additive increase and multiplicative decrease (AIMD) congestion control scheme are modeled based on stochastic network calculus (SNC). Particularly, the probabilistic bounds are modeled through moment generating function (MGF)-based SNC with regard to the sending rate distribution of CR source sensors. The proposed stochastic bounds are verified through NS2-based simulations.

Keywords: Stochastic network calculus, backlog bound, delay bound, cognitive radio sensor networks, rate-based congestion control, AIMD

1. Introduction

Inefficient usage of spectrum in traditional wireless networks has lead to use of dynamic spectrum access (DSA) solutions. Cognitive radio (CR) technology is a capable tool to provide DSA and significantly improve performance and spectral efficiency in the next generation wireless networks [1]. A wireless network with CR-equipped nodes is called a cognitive radio network (CRN) [2]. A CR node senses the spectrum channels to find some vacant channels, i.e., the channels that are not occupied by primary users (PUs). Primary users in CRNs are the licensed users that have higher priority to use the licensed channels and

Email addresses: v_esmaeelzadeh@iust.ac.ir (Vahid Esmaeelzadeh),
rberangi@iust.ac.ir (Reza Berangi), elahe_hosseini@iust.ac.ir (Elahe S. Hosseini),
akan@ku.edu.tr (Ozgur B. Akan)

CR users can only use the licensed channels in the absence of PUs. After spectrum sensing, the CR node selects an appropriate channel among the vacant channels in order to data transmission (spectrum decision) and if it is needed, a spectrum handoff is occurred (spectrum mobility). Since a CR node senses the channels periodically, if a PU enters into its licensed channel, the CR node detects the presence of PU and leave the channel immediately in order to minimize the interference on the transmission of PUs [2]. Cognitive radio is widely used in the different types of traditional wireless networks. Using of CR in traditional wireless sensor networks (WSNs) defines a new type of wireless networks called cognitive radio sensor networks (CRSNs) [3]. The DSA capability of CR sensors can reduce the collision, congestion and retransmission probabilities in the applications of WSNs with bursty traffic. Moreover, opportunistic spectrum access of CR sensors improves the transmission efficiency which leads to save and reduce the power consumption of resource-limited sensors in CRSNs [3].

The dynamicity of available bandwidth in CRSNs because of PUs' activity and the operations of spectrum sensing and handoff, has crucial impacts on the performance of MAC, network and transport layer protocols. The main objective of CRSNs cannot be appropriately realized if the effects of unique features of CRSNs are not considered in the evaluation and the tuning of the parameters of different layers protocols. Hence, the performance evaluation of the protocols based on the CR-related parameters is critical in order to provide the quality of service (QoS) objectives in CRSNs. In this paper, we focus on the performance of congestion control schemes in CRSNs.

Providing the transport layer-based QoS can be important in various applications of CRSNs. The performance metrics of transport layer should be studied and modeled to satisfy various QoS guarantees in CRSNs. There are some studies [4, 5, 6, 7, 8, 9, 10, 11, 12, 13] about the performance evaluation of transport layer in CRSNs and CRNs. Most of these papers evaluate the performance of transport layer protocols in CRNs and CRSNs based on simulations. In [14], the sending rate distribution of rate-based congestion control schemes is modeled in CRSNs. The [15] investigates the optimality of rate-based AIMD and AIAD congestion control schemes in CRSNs. However, there is no analytical modeling of rate-based congestion control schemes in the terms of stochastic backlog and delay bounds in CRSNs.

Stochastic network calculus (SNC) is a min-plus algebra based theory in order to model the probabilistic backlog and delay bounds of different network elements [16]. SNC is originated from its deterministic version as introduced by Cruz [17, 18] and is developed in [19]. There are some SNC-based performance evaluation studies in CRNs [20, 21, 22, 23, 24]. However, there is no SNC-based study on the congestion control schemes in CRNs and CRSNs. Modeling the stochastic backlog and delay bounds of rate-based congestion control schemes based on the SNC can be used to provide QoS in various applications of CRSNs. To the best of our knowledge, there is no modeling of stochastic delay and backlog bounds of rate-based congestion control schemes for CRSNs based on SNC in the current literature. Among the rate-based schemes, we focus on the popular one, i.e., generic additive increase multiplicative decrease (AIMD)

[25]. In this paper, the stochastic backlog and delay bounds of rate-based generic AIMD congestion control scheme are modeled in CRSNs. The stochastic bounds are modeled through moment generating function (MGF)-based SNC [26] based on our previous work on the modeling of the sending rate distribution of CR source sensors in CRSNs [14]. The proposed bounds are verified through various NS2-based simulations.

In the rest of paper, the system model of CRSN is described in Section 3. Section 4 explains the sending rate distribution of CR source sensors. The stochastic backlog and delay bounds are modeled in Section 5. Analytical results and simulation-based verifications are presented in Section 6. Finally, we conclude the paper in Section 7.

2. Related Work

To the best of our knowledge, there is no modeling of stochastic backlog and delay bounds of rate-based congestion control schemes for CRSNs and CRNs based on stochastic network calculus. In [4], the impacts of CR-related parameters on the performance of congestion control schemes are investigated in CRSNs. The challenges of real-time transport over CRSNs in various spectrum environments of smart grid applications are studied in [5]. The throughput and efficiency of TCP protocol in CRNs are investigated simulation-based in [6]. Authors in [7] study the impact of PU' activity, spectrum sensing time and the number of wireless channels on the TCP throughput. In [8], the behavior of TCP throughput, the size of congestion window and the value of round trip time (RTT) are studied with regard to the heterogeneity of spectrum channels, the spectrum sensing frequency, PU' traffic. In [9], the impact of spectrum sensing time and the changes of the available bandwidth of CR nodes on the behavior of TCP congestion control are studied. A study on the TCP performance degradation in CRNs with regard to the congestion window size, RTT behavior and retransmission timeout (RTO) is done in [10]. In [11], based on the PU' activity and the number of available wireless channels, the performance of TCP throughput is evaluated. An equation-based transport protocol for CRNs is introduced in [12]. Authors in [13] investigate on the TCP end-to-end delay, throughput and packet drop probability with regard to the packet size and various CR-related parameters. However, most of these studies investigate the performance evaluation of transport layer in CRNs and CRSNs based on simulation and there is no analytical modeling of rate-based congestion control schemes.

Some researchers study on the performance evaluation modeling based on stochastic network calculus in CRNs. In [20], the effects of spectrum sensing errors and various retransmission schemes in CRNs are investigated based stochastic network calculus. In this study, the backlog and delay bounds for primary and secondary users are modeled. The authors of [21] propose a stochastic arrival curve for spectrum sensing error process and a stochastic service curve for a Gilbert-Elliott fading wireless channel in CRNs. Based on the proposed arrival and service curves, the capacity limits of CRNs under wireless fading

channel are modeled. The [22] proposes an SNC-based approach to find the capacity of CRNs under the period and Poisson traffic types with delay constraints. In [23, 24], the delay bounds for cognitive radio users and primary users in CRNs with parallel Markov modulated On-Off channels are analyzed based on stochastic network calculus. However, there is no stochastic backlog and delay bounds modeling of rate-based congestion control schemes in CRSNs and CRNs.

In [14], the sending rate distribution of rate-based congestion control schemes in CRSNs is modeled based on a semi-Markov chain and the congestion probability of network. The congestion probability of network is calculated based on the proposed models of the queue length distribution and delay overhead of MAC layer. In [15], the optimality of rate-based congestion control schemes is investigated in CRSNs. In this study, the optimal rate-based congestion control schemes are obtained in order to maximize the new defined metric called Rate-Congestion Ratio (RCR). The maximization of the RCR leads to maximize the mean sending rate of congestion control scheme and minimize the congestion probability of network simultaneously. However, the stochastic delay and backlog bounds of rate-based congestion control schemes in CRSNs are not considered.

3. System Model

In wireless sensor networks, breaking the low quality and long distance wireless links into multiple short distance and high quality links is a usual strategy in order to facilitate the event delivery from source sensor nodes to the sink station. Such breaking the links is done through relay nodes. Using the relay nodes in multiple hops can decrease the path loss and increase the lifetime of power supply-limited sensor nodes in WSNs [27].

In our analysis, a cognitive radio sensor network is composed of several CR source sensors and CR relay nodes in multiple hops. Forwarding the sensed data from CR source sensors toward the sink station is done through the CR relay nodes. The relay nodes can be grouped into multiple groups based on the their distance from the sink and source sensor nodes. Fig. 1 illustrates the CRSN model. The network consists of three types of nodes: CR source sensor nodes, CR relay nodes and the sink station. The CR relay nodes are grouped into H hops and the number of relay nodes at hop h is denoted by N_h . The number of source nodes in the event area is N_0 that sense the area in order to send some information toward the sink station.

Each CR node has two main modes, spectrum sensing mode and data transmission mode, that switches between these modes periodically. In the spectrum sensing mode, a CR node senses the licensed spectrum to detect the activity of primary users (PUs). The duration of being in spectrum sensing mode is called sensing time and is denoted by t_s . It is assumed that sensing is done ideally and there is no sensing error. Spectrum sensing is done periodically with the period of τ . After spectrum sensing, the CR node enters into the data trans-

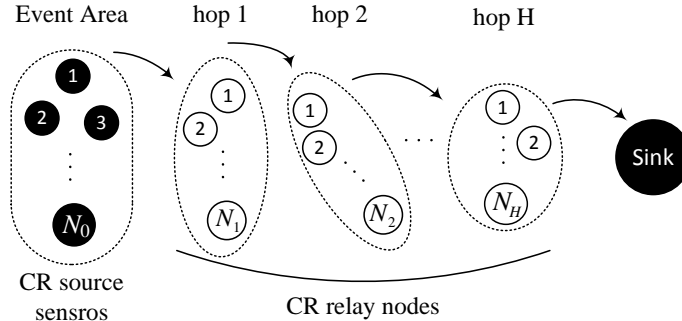


Figure 1: CRSN model. CR source sensor nodes send data through the CR relay nodes toward the sink station. Primary users' activity affect the data communication of CR nodes at each hop in the wireless channels.

mission mode and transmit data on a vacant channel for the duration of data transmission $t_d = \tau - t_s$.

The activity of primary users can be modeled by a two-state birth/death process with the mean birth rate of β and mean death rate of α [28]. The birth rate is equivalent to the entrance rate (β) of PUs in their licensed channels. Also, the death rate is equivalent to the departure rate (β) of PUs from their licensed wireless channels. A separate and independent primary user operates at each wireless channel based on the traffic model of PUs.

A congestion control scheme is composed of three main units: congestion detection, congestion notification and congestion avoidance [29]. Congestion detection is the detection of some events which may cause congestion in the network. In the literature, several events such as queue length, packet rate, node delay, channel status and reliability parameters are used to detect the congestion in WSNs [29]. In this paper, the queue length of nodes (most used congestion detection parameter in congestion control schemes) is assumed as the congestion detection parameter. It is assumed the congestion notification is done ideally without any packet loss from the sink station toward the source nodes. Usually, the congestion avoidance is done through rate adjustment algorithms in WSNs. Regulating the sending rate of source sensors based on the reception of congestion notification is called rate adjustment. There are two basic types of rate adjustment algorithms [29]: simple rate adjustment and exact rate adjustment. In the simple rate adjustment algorithms, the rate adjusting is done based on a single congestion bit. The additive increase multiplicative decrease (AIMD) scheme is one of the popular variations of simple rate adjustments. In the exact rate adjustments, the rate adjusting operation is performed based on the exact congestion level of the network. In this paper, we consider the generic AIMD rate adjustment as the congestion avoidance scheme which

is executed in the sink station. The rate adjusting decisions are made in the sink station and sent to the CR source sensors periodically with a predefined constant period. The minimum value of the adjusted rate is assumed one packet per time unit. We assume that the CR source sensors have a higher bound of R packets per time unit on their sending rate because of the limitations of the sink station. In many applications of sensor networks, the sensor nodes generate and send constant bit rate (CBR) data toward the sink station such as environmental monitoring and data gathering [30]. Hence, the application layer sending rate of CR source sensors is considered constant bit rate with the rate of R_a packet per time unit.

4. The steady-state sending rate distribution of a CR source sensor in CRSNs

The sending rate of a generic rate-based AIMD scheme is adjusted as follows [14]

$$r(t+1) = \begin{cases} \max(1, \lfloor \frac{r(t)}{DEC} \rfloor) & \text{with probability } \Omega_{r(t)} \\ \min(r(t) + INC, R) & \text{with probability } 1 - \Omega_{r(t)} \end{cases} \quad (1)$$

where $t \in \{0, 1, 2, \dots\}$ is the discrete time instances; the $r(t) \in \{1, 2, \dots, R\}$ is the adjusted sending rate of sources at time t and $\Omega_{r(t)}$ is the congestion probability in the shared portion of network between the source nodes and the sink station while the source nodes are sending with the rate $r(t)$. The congestion probabilities are calculated in our previous work [14] for CRSNs. The $r(t+1)$ is the new adjusted sending rate of the source nodes. The AIMD scheme increases the sending rate additively by INC factor if there is no congested node in the network at the duration of one time unit and decreases the sending rate multiplicatively by DEC if at least a congestion is detected. The AIMD schemes with the INC and DEC factors are represented by AIMD(INC,DEC).

Based on the Equ. 1, the AIMD scheme is at one of the states $\{z_1, z_2, \dots, z_R\}$. For each state z_i ($i \in \{1, 2, \dots, R\}$), the $r_{z_i} = i$ is the regulated sending rate of scheme at state z_i . A CR source sensor sends with each regulated rate for the duration of one time unit. Therefore, the sojourn time of being in the various states is constant value of one time unit. Consequently, we model the AIMD scheme state process $Z(t)$ by a semi Markov chain (SMC) with the states $\{z_1, z_2, \dots, z_R\}$ and transition probability matrix $\mathbf{T}_{R \times R}$ where R is the number of states. The $T_{z_i, z_{i^*}}$ is the state transition probability from the state z_i to the state z_{i^*} . This matrix is constructed with regard to the values of congestion probabilities (Ω_i). For the AIMD(INC,DEC) scheme, the elements of transition matrix $\mathbf{T}_{R \times R}$ are

$$\begin{aligned} T_{z_i, z_{\min\{i+INC, R\}}} &= 1 - \Omega_i & \forall i \in \{1, 2, \dots, R\} \\ T_{z_i, z_{\max\{\lfloor i/DEC \rfloor, 1\}}} &= \Omega_i & \forall i \in \{1, 2, \dots, R\}. \end{aligned} \quad (2)$$

The embedded DTMC of an SMC is obtained when the behavior of the SMC is observed at the discrete instances that the state transitions occur [31]. The

embedded DTMC of the proposed SMC is a finite state, aperiodic, irreducible Markov chain; hence a unique steady-state distribution can be found for this embedded DTMC [31]. Based on the DTMC, we have a system of linear equations with R independent equations and R unknown variables. By solving the linear equations system, the steady state distribution of the embedded DTMC, i.e., $\mathbf{P} = (P_1, P_2, \dots, P_R)$, is obtained.

The sojourn time of all states are equal to one time unit because the sending rate is adjusted to new value at each time unit, i.e., $T_{z_1} = T_{z_2} = \dots = T_{z_R} = 1$ time unit where T_{z_i} is the sojourn time of the state z_i . Therefore, the steady state distribution of SMC is equal to the steady state distribution of embedded DTMC because

$$\pi_i = \frac{P_i T_{z_i}}{\sum_{i=1}^R P_i T_{z_i}} = \frac{P_i T_{z_i}}{T_{z_i}} = P_i \quad i = 1, 2, \dots, R \quad (3)$$

where $\mathbf{P} = (P_1, P_2, \dots, P_R)$ is the steady state distribution of embedded DTMC and $\boldsymbol{\pi} = (\pi_1, \pi_2, \dots, \pi_R)$ is the steady state distribution of SMC. Since the regulated sending rate of a CR source sensor at state z_i is i packets per time unit, i.e., $r_{z_i} = i$, the $\boldsymbol{\pi} = (\pi_1, \pi_2, \dots, \pi_R)$ is equivalent to the sending rate distribution of source nodes.

5. Stochastic backlog and delay bounds

In this section, the stochastic backlog and delay bounds of rate-based AIMD congestion control scheme are modeled based on the stochastic network calculus. The bounds are modeled based on the sending rate distribution of source nodes.

The basic theories of stochastic network calculus [16] model the backlog and delay bounds of a server based on the stochastic service curve and arrival curve of the server. A rate-based congestion control scheme can be considered as a server that its service rate is equivalent to its adjusted sending rate. Hence, we have the service rate distribution of a server instead of its service curve. Consequently, we can use the MGF-based backlog and delay bound theories. In [26], backlog and delay bounds are calculated based on the moment generating functions (MGF) of arrival process and service process. In Subsection 5.1, the related definitions and theories are explained.

5.1. Basic Definitions and Theories

Definition 1. The (cumulative) arrival process of a server is denoted by $A(0, t)$ which is the (cumulative) amount of traffic (in the number of packets) arriving at server in the time interval $[0, t]$ [16].

Definition 2. The (cumulative) service process of a server is denoted by $S(0, t)$ which is the (cumulative) amount of service provided (in the number of packets) by the server in the time interval $[0, t]$ [16].

Definition 3. The moment generating functions (MGFs) of $A(0, t)$ and $S(0, t)$ are defined as [16]

$$M_A(\theta, t) = E[e^{\theta A(0,t)}] \quad \forall \theta \in (0, \infty) \quad (4)$$

$$M_S(\theta, t) = E[e^{\theta S(0,t)}] \quad \forall \theta \in (0, \infty) \quad (5)$$

where $E[X]$ is the expectation of random process X .

Let us explain more in detail how to calculate the MGF of a cumulative process. Suppose that the cumulative process $S(0, t)$ has a finite number of values $s_1 < s_2 < \dots < s_k$ with the probabilities $p_1(t), p_2(t), \dots, p_k(t)$ for the interval $[0, t]$. The value of $E[e^{\theta S(0,t)}]$ is calculated as follows:

$$M_S(\theta, t) = E[e^{\theta S(0,t)}] = \sum_{i=1}^k p_i(t) e^{\theta s_i}. \quad (6)$$

Theorem 1. The stochastic backlog and delay bounds of a server with cumulative arrival process $A(0, t)$ and cumulative service process $S(0, t)$ are (arrival and service processes are statistically independent and stationary) [26, 32]

$$P(b(t) > B) \leq e^{-\theta B} \sum_{s=0}^{\infty} M_A(\theta, s) M_S(-\theta, s) \quad \forall \theta \in (0, \infty) \quad (7)$$

$$P(d(t) > D) \leq \sum_{s=D}^{\infty} M_A(\theta, s - D) M_S(-\theta, s) \quad \forall \theta \in (0, \infty) \quad (8)$$

where $b(t)$ and $d(t)$ are the amounts of backlog and delay at time $t \geq 0$ respectively. Also, the $M_A(\theta, s)$ and $M_S(\theta, s)$ are the moment generating functions of $A(0, s)$ and $S(0, s)$ respectively (The Appendix section provides the proof of this theory).

5.2. Backlog and delay bounds of generic AIMD congestion control scheme

The block diagram of a rate-based AIMD congestion control scheme as a server with its arrival process $A(0, t)$ and service process $S(0, t)$ is depicted in Fig. 2. A CR source sensor adjusts its rate based on the AIMD congestion control scheme and the received congestion notification from the sink node with regard to Equ. 1.

It is assumed that CR source sensors generate and send constant bit rate (CBR) data with the rate of R_a packets per time unit [30]. Hence, we have

$$\begin{aligned} A(0, t) &= R_a t \\ M_A(\theta, t) &= e^{\theta R_a t}. \end{aligned} \quad (9)$$

Recall that a rate-based AIMD scheme is modeled as a server so that its service is the sending of packets. The states process of an AIMD scheme, i.e.,

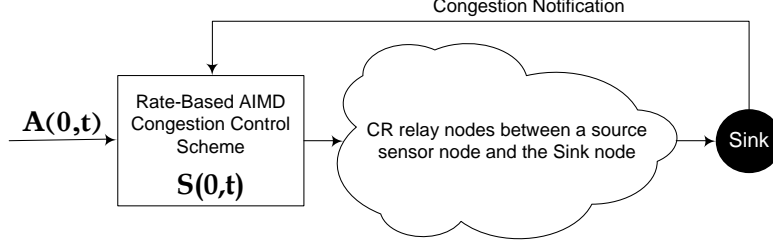


Figure 2: Rate-based AIMD congestion control scheme. The $A(0,t)$ and $S(0,t)$ are the arrival process and service process of congestion control scheme respectively. A CR source sensor adjusts its rate with regard to AIMD scheme and the received congestion notification from the sink node.

$Z(t)$, is modeled by an SMC with transition probability matrix $\mathbf{T}_{R \times R}$ and steady state distribution vector $\boldsymbol{\pi} = (\pi_1, \pi_2, \dots, \pi_R)$ where $Z(t) = z_i$ if the state of AIMD scheme is z_i at time t . Hence, the AIMD scheme states process $Z(t)$ is a homogeneous Markov process with transition probability matrix \mathbf{T} and steady state distribution vector $\boldsymbol{\pi}$. Also, the sending rate of AIMD scheme (the service rate of server) at state z_i is $r_{z_i} = i$ packets per time unit; therefore, the sending rate process $r(t) = r_{Z(t)}(t)$ is a Markov modulated process [31]. The sending rate process, i.e., the service rate of server, can be calculated as follows

$$\begin{aligned}
 S(0, t) &= S(0, 1) + S(1, 2) + \dots + S(t-1, t) \\
 &= r(1) + r(2) + \dots + r(t) \\
 &= \sum_{t'=1}^t r(t')
 \end{aligned} \tag{10}$$

and the value of $M_S(\theta, t)$ can be calculated through Theorem 2.

Theorem 2. Let $Z(t)$ be a homogeneous Markov process of states $\{z_1, z_2, \dots, z_R\}$ with transition probability matrix \mathbf{T} and steady state distribution vector $\boldsymbol{\pi}$. For the Markov modulated process $r(t) = r_{Z(t)}(t)$, the MGF of $S(0, t) = \sum_{t'=1}^t r(t')$ is obtained by [33]

$$\begin{aligned}
 M_S(\theta, 0) &= 1 \\
 M_S(\theta, t) &= \boldsymbol{\pi}(\mathbf{V}(\theta)\mathbf{T})^{t-1}\mathbf{V}(\theta)\mathbf{1}_R \quad \forall t \in \{1, 2, 3, \dots\}
 \end{aligned} \tag{11}$$

where $\mathbf{V}(\theta)$ is a diagonal matrix that is obtained as follows

$$\mathbf{V}_{R \times R}(\theta) = \text{diag}(e^{\theta r_{z_1}}, e^{\theta r_{z_2}}, \dots, e^{\theta r_{z_R}}) \quad \forall \theta \in (0, \infty) \tag{12}$$

and $\mathbf{1}_R$ is a column vector with all its R elements equal to one.

Let $\epsilon \in (0, 1]$ be the permissible probability that the backlog and delay violate the desired bounds, i.e., $P(b(t) > B) \leq \epsilon$ and $P(d(t) > D) \leq \epsilon$. With regard to Theorem 1 and Theorem 2, the backlog and delay bounds of the rate-based AIMD scheme are calculated as follows [32]

$$B = \inf_{\theta > 0} \left\{ \frac{1}{\theta} \left(\ln \sum_{s=0}^{\infty} M_A(\theta, s) M_S(-\theta, s) - \ln \epsilon \right) \right\} \quad (13)$$

$$D = \inf_{\theta > 0} \left\{ \inf \left\{ \tau : \frac{1}{\theta} \left(\ln \sum_{s=\tau}^{\infty} M_A(\theta, s - \tau) M_S(-\theta, s) - \ln \epsilon \right) \leq 0 \right\} \right\} \quad (14)$$

where $M_A(\theta, s)$ and $M_S(-\theta, s)$ are obtained through the Equ. 9 and Equ. 11 respectively. To calculate the value of $M_S(-\theta, s) = \boldsymbol{\pi}(\mathbf{V}(-\theta)\mathbf{T})^{s-1}\mathbf{V}(-\theta)\mathbf{1}_R$, the values of \mathbf{T} elements are obtained by Equ. 2. Also, the $\boldsymbol{\pi}$ is obtained by calculating the steady state distribution of the proposed SMC in Section 4. Since $r_{zi} = i$ packets per time unit for all $i \in \{1, 2, \dots, R\}$, the matrix $\mathbf{V}(-\theta) = \text{diag}(e^{-\theta}, e^{-2\theta}, \dots, e^{-R\theta})$.

6. Simulation results and verifications

The proposed models of stochastic backlog and delay bounds are verified using simulations through CogNS simulation framework [13] that is a simulation framework for cognitive radio networks based on Network Simulator 2 (NS2) [34]. In this way, we have developed the rate-based congestion control schemes in the transport layer of the CogNS framework.

6.1. Simulation settings

Simulation settings and the CRSN parameters are summarized in Table 1. The CRSN area is $500 \times 500 \text{ m}^2$. The network consists of 6 CR source sensors and 12 CR relay nodes (in 4 hops with 3 nodes at each hop) and a sink station. The number of wireless channels is 6 with the same bandwidth of 1 Mbps. One primary user per channel operates with the entrance rate (β) and the departure rate (α). The values of α and β are varied in various experiments. The data transmission duration (t_d) of CR nodes are 1 second and the value of sensing time (t_s) is varies in various simulations. A simple CSMA/CA-base multichannel protocol is considered as MAC protocol. The routing protocol and queue management strategy are the AODV protocol and the droptail strategy respectively. The generic rate-based AIMD scheme is considered as transport protocol. The packet size is set to 120 bytes. The time unit of AIMD scheme, i.e., congestion notification period of sink station, is set to 1 second. The maximum sending rate of AIMD scheme (R) is 200 packets per second. The INC and DEC factor of AIMD scheme are varies in various experiments. The queue size

Table 1: CRSN configuration and simulation settings

Parameter	Value/type
Network area	$500 \times 500 m^2$
Nodes spatial distribution	$H = 4, N_0 = 6,$ $N_1 = N_2 = N_3 = N_4 = 3$
The number of wireless channels	6
The bandwidth of wireless channels	1 Mbps
PUs' activity (α, β)	variable in different experiments
Sensing time (t_s)	variable in different experiments
Operating time (t_o)	1 sec
MAC protocol	Simple CSMA/CA-based multichannel protocol
Routing protocol	Ad-hoc On-demand Distance Vector (AODV)
Queue management strategy	Droptail
Transport protocol	Generic rate-based AIMD scheme
Rate adjustment factors (INC,DEC)	variable in different experiment
Unit time of AIMD scheme	1 sec
Permissible probability that the backlog and delay violate the desired bounds (ϵ)	0.01
Packet size	120 bytes
Maximum allowable sending rate (R)	200 packets/sec
Queue size	100 packets
The queue length threshold for congestion detection	90 packets
The traffic rate of application layer (R_a)	variable in different experiments

of nodes is 100 packets and the queue length threshold for the detection of congestion is 90 packets. The traffic rate of application layer (R_a) is varies in different experiments. The permissible probability that the backlog and delay of AIMD scheme violate the desired bounds, i.e., ϵ , is determined 0.01.

6.2. Verification of backlog and delay bounds models

To verify the backlog and delay bounds, it is needed to compare the analytical results with simulation results for different experiments. Table 2 shows the parameters of four experiments which are considered to present the verification of the backlog and delay bounds models. The traffic rate of application layer (R_a), the sensing time of CR nodes (t_s), the activity parameters of primary users (α, β) and the rate adjustment factors of AIMD scheme (INC,DEC) are considered as variable parameters in the experiments I, II, III, IV respectively. In these experiments, the values of other parameters are set as denoted in Table 1.

Table 2: Different experiments to present the verification of backlog and delay bounds models

Exp. #	R_a [packets per second]	t_s [second]	(α, β)	(INC,DEC)
I	{37, 40, 43, 46, 49, 52, 55}	0.1	(3,1)	(1,3)
II	40	{0.02, 0.1, 0.2, 0.3, 0.4, 0.5}	(3,1)	(1,3)
III	36	0.1	{(5,1), (3,1), (1,1), (1,3), (1,5)}	(1,3)
IV	50	0.1	(3,1)	{(1,4), (1,3), (1,2), (2,2), (3,2), (4,2)}

In the experiment I, the backlog and delay bounds are verified and investigated for different values of application layer traffic rate $R_a \in \{37, 40, 43, 46,$

49, 52, 55} packets per second. In the experiment II, for the various values of sensing time $t_s \in \{0.02, 0.1, 0.2, 0.3, 0.4, 0.5\}$ second, the values of backlog and delay bounds are studied and verified. Different values of PUs' entrance and departure rates $(\alpha, \beta) \in \{(5,1), (3,1), (1,1), (1,3), (1,5)\}$ are considered in the experiment III. Experiment IV investigates the values of delay and backlog bounds for different AIMD schemes with factors $(\text{INC}, \text{DEC}) \in \{(1,4), (1,3), (1,2), (2,2), (3,2), (4,2)\}$. The sensing time is set to 0.1 second for the experiments I, III, IV. The primary users' activity is considered as $(\alpha, \beta) = (3, 1)$ for the experiments I, II, IV. The AIMD(1,3) scheme is considered in the experiments I, II, III. The application layer traffic rate is set to 40, 36 and 50 packets per second in the experiments II, III and IV respectively. Recall that, in all experiments, the value of ϵ (the permissible probability that the backlog and delay violate the desired bounds) is set to 0.01. Hence, the stochastic backlog (B) and delay (D) bounds are defined as $P(b(t) > B) \leq \epsilon = 0.01$ and $P(d(t) > D) \leq \epsilon = 0.01$ respectively. The simulation-based and model-based results of experiments I, II, III and IV are presented in figures 3, 4, 5 and 6 respectively.

By increasing the application layer traffic rate (increasing the arrival traffic of AIMD server), the backlog and delay bounds increase. In Fig. 3(a) and Fig. 3(b), the stochastic backlog and delay bounds of AIMD(1,3) scheme which are obtained from the simulations are compared with those obtained from the proposed backlog and delay bounds models. In Fig. 3(a), the value of stochastic backlog bound B is depicted for various values of R_a . The model-based values of B are calculated 35, 65, 104, 152, 209, 275 and 350 packets and the simulation-based values are obtained 25, 51, 81, 130, 180, 253 and 345 packets for the values of $R_a \in \{37, 40, 43, 46, 49, 52, 55\}$ packets per second respectively that verify the backlog bound model. Also, in Fig. 3(b), the stochastic delay bound D is illustrated for different values of R_a . Based on the model of delay bound (Equ. 14), the value of D is calculated 1, 2, 3, 4, 5, 6 and 7 second(s) for the considered values of R_a respectively. The obtained delay bounds through simulations are 0.97, 1.37, 2.44, 3.32, 4.28, 4.86 and 6.38 second(s) for the values of R_a respectively that verify the delay bound model.

The increase of the sensing time increases the backlog and delay bounds; because the increase of sensing time leads to more delay overhead of nodes MAC layer; hence, the congestion probability of network nodes increase. Consequently, the adjusted sending rate of AIMD scheme (service rate of AIMD server) is reduced that leads to the increasing of backlog and delay bounds of AIMD scheme. In Fig. 4(a), the value of stochastic backlog bound B is depicted for different values of t_s . The analytical values of B are calculated 48, 65, 91, 136, 162 and 171 packets and the simulation-based values are 40, 51, 90, 127, 150 and 165 packets for the values of $t_s \in \{0.02, 0.1, 0.2, 0.3, 0.4, 0.5\}$ second respectively that that verify the backlog bound model. Also, in Fig. 4(b), the stochastic delay bound D is illustrated for different values of t_s . The analytical value of D is calculated 2, 2, 3, 4, 5 and 5 second(s) for the values of $t_s \in \{0.02, 0.1, 0.2, 0.3, 0.4, 0.5\}$ second respectively. The obtained delay bounds through simulations are 1.12, 1.37, 2.27, 3.3, 3.82 and 4.22 seconds for the considered

values of t_s respectively that verify the proposed delay bound.

By increasing the activity of primary users, the available bandwidth of wireless channels decreases for CR nodes. Therefore, the congestion probability of CR nodes is raised that leads to the decreasing of the adjusted rate of AIMD scheme. Consequently, we have greater backlog and delay bounds. In Fig. 5(a), for different values of (α, β) , the values of stochastic backlog bound B are depicted. The calculated values of backlog bound B based on the proposed model are calculated 19, 25, 31, 83 and 147 packets for the value $(\alpha, \beta) \in \{(5,1), (3,1), (1,1), (1,3), (1,5)\}$ respectively. The values of backlog bounds through simulations are obtained 15, 20, 28, 66 and 135 packets for the considered values of PUs' activity that verify the stochastic backlog bound model. Also, in Fig. 5(b), the values of stochastic delay bound D are illustrated for the various values of (α, β) . The D is analytically calculated 1, 1, 1, 3 and 5 second(s) and is obtained 0.42, 0.58, 0.77, 2.16 and 3.77 seconds based on simulation for the values of $(\alpha, \beta) \in \{(5,1), (3,1), (1,1), (1,3), (1,5)\}$ respectively. The obtained results verify the stochastic delay bound model.

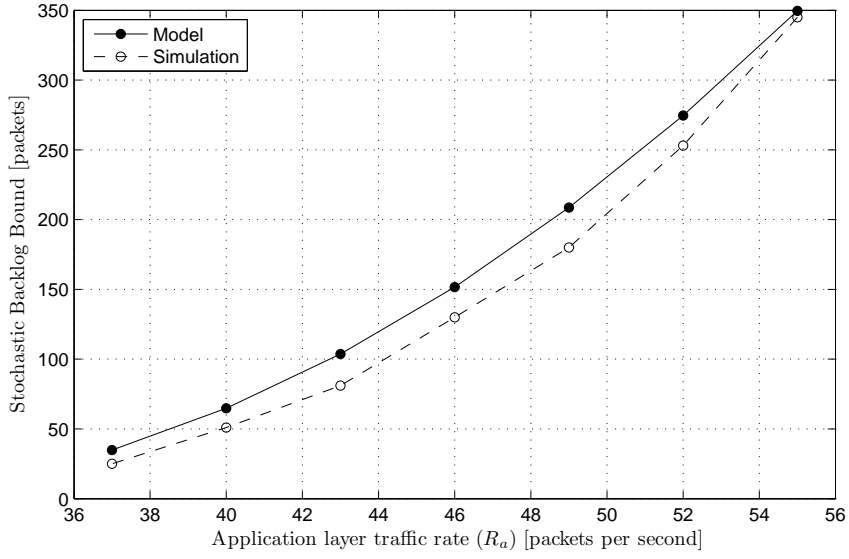
Increasing the INC factor and decreasing the DEC factor of AIMD scheme raise the adjusted rate of AIMD scheme (service rate of AIMD server). Hence, the backlog and delay bounds will be smaller. In Fig. 6(a), the values of stochastic backlog bound B are depicted for various AIMD schemes. The model-based values of B are calculated 415, 227, 29, 11, 7 and 6 packets and the simulation-based backlog bounds are obtained 368, 214, 17, 5, 4 and 2 packets for the AIMD schemes with factors $(\text{INC}, \text{DEC}) \in \{(1,4), (1,3), (1,2), (2,2), (3,2), (4,2)\}$ respectively that verify the backlog bound model. In Fig. 6(b), the stochastic delay bound D is illustrated for different AIMD schemes. The model-based values of D are calculated 9, 5, 1, 1, 1 and 1 second(s) and the simulation-based values are obtained 7.6, 4.51, 0.56, 0.12, 0.08 and 0.06 second(s) for the AIMD schemes with factors $(\text{INC}, \text{DEC}) \in \{(1,4), (1,3), (1,2), (2,2), (3,2), (4,2)\}$ respectively that verify the delay bound model.

7. Conclusions

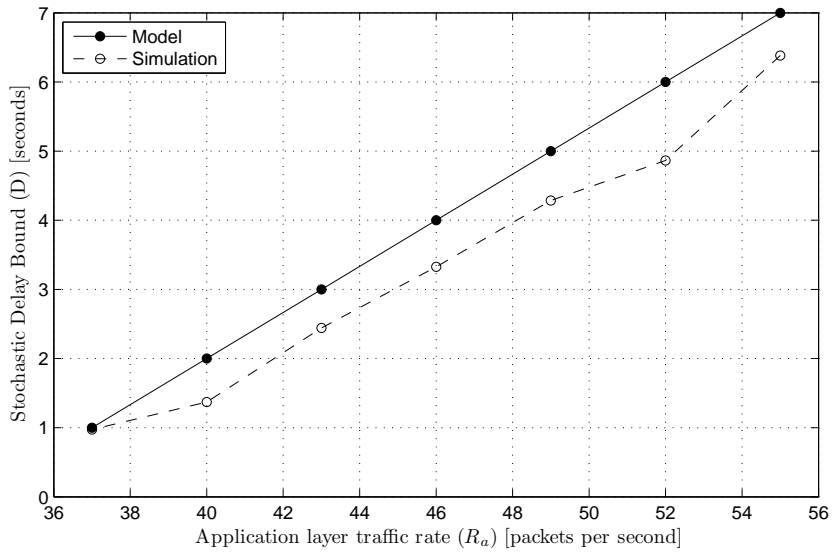
In this paper, the performance of rate-based AIMD congestion control scheme has been evaluated based on the stochastic network calculus (SNC). In this way, the stochastic backlog and delay bounds have been modeled based on the sending rate distribution of CR source sensors using the moment generating function (MGF)-based SNC. The proposed probabilistic bounds have been verified through several NS2-based simulations. Future study in this research field can be the finding of optimal AIMD congestion control schemes in order to minimize the backlog and delay bounds and congestion probability for CRSNs in various applications.

8. Appendix

Proof of Theorem 1 [32]: For a server with arrival process $A(0,t)$ and service process $S(0,t)$ that are statistically independent and stationary, the stochastic

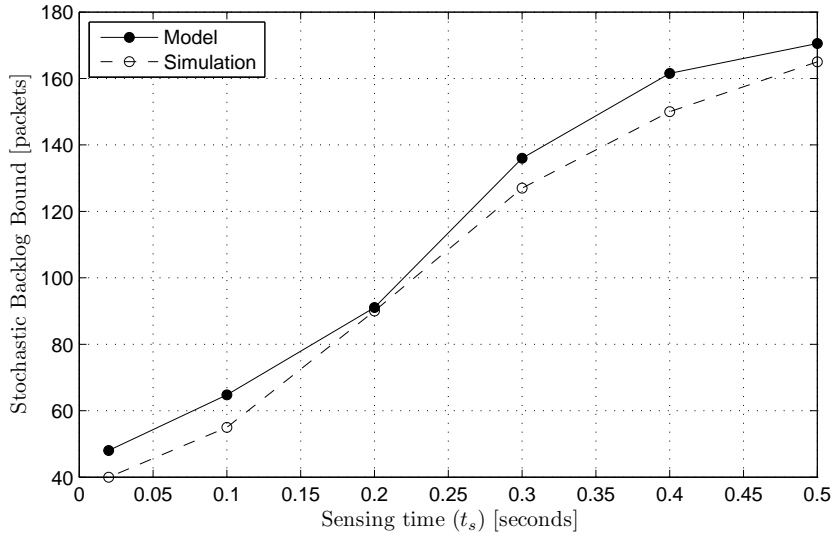


(a) Stochastic backlog bound (B) vs. application layer traffic rate (R_a)

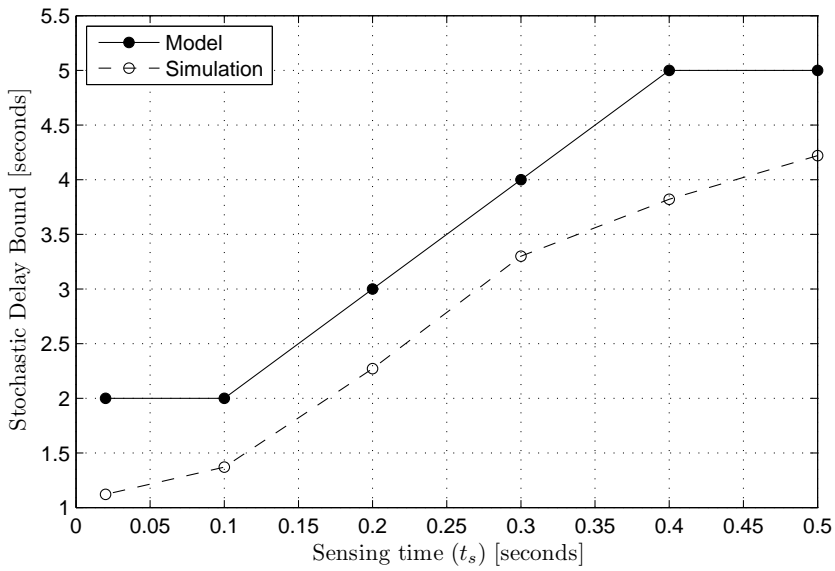


(b) Stochastic delay bound (D) vs. application layer traffic rate R_a

Figure 3: The verification of stochastic backlog and delay bounds models by the simulations in the experiment I

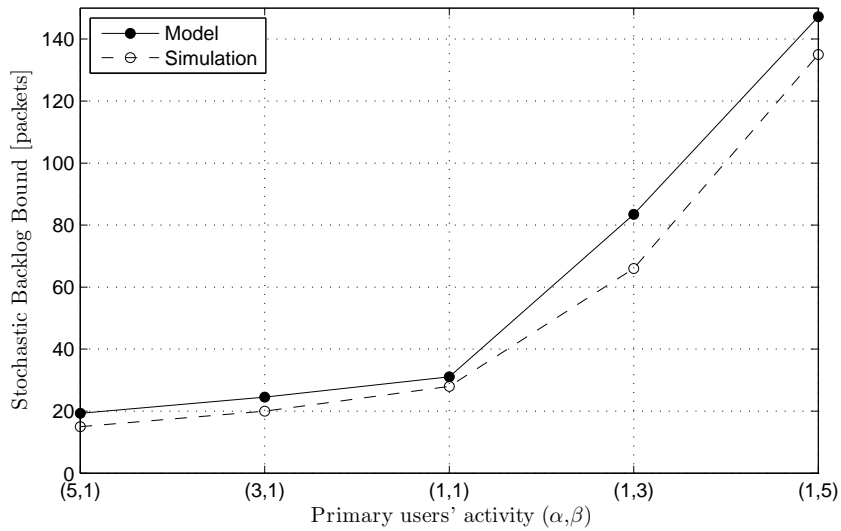


(a) Stochastic backlog bound (B) vs. sensing time (t_s)

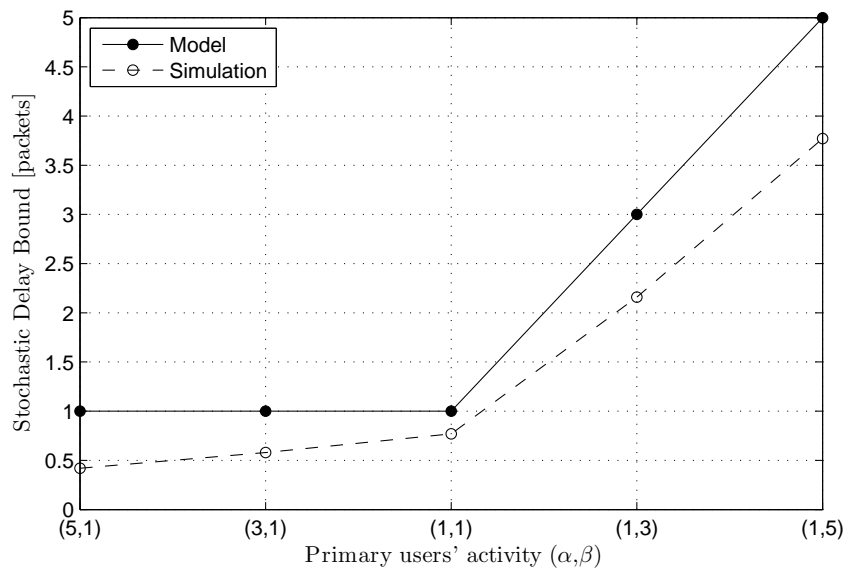


(b) Stochastic delay bound (D) vs. sensing time t_s

Figure 4: The verification of stochastic backlog and delay bounds models by the simulations in the experiment II

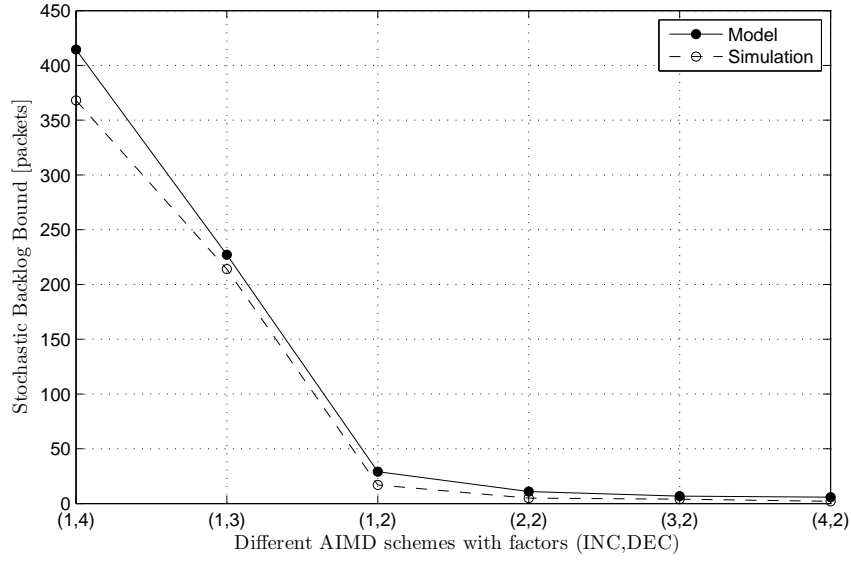


(a) Stochastic backlog bound (B) vs. the activity of PUs (α, β)

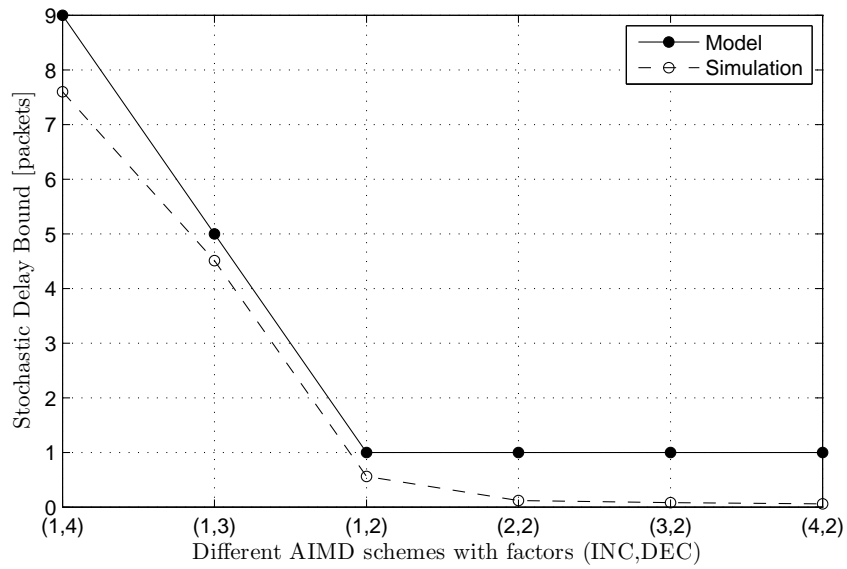


(b) Stochastic delay bound (D) vs. the activity of PUs (α, β)

Figure 5: The verification of stochastic backlog and delay bounds models by the simulations in the experiment III



(a) Stochastic backlog bound (B) vs. AIMD (INC,DEC) schemes



(b) Stochastic delay bound (D) vs. AIMD (INC,DEC) schemes

Figure 6: The verification of stochastic backlog and delay bounds models by the simulations in the experiment IV

delay and backlog bounds are calculated as follows [16]:

$$P\{b(t) > B\} \leq P\left\{\max_{0 \leq s \leq t} \{A(s, t) - S(s, t)\} > B\right\} \quad (15)$$

$$P\{d(t) > D\} \leq P\left\{\max_{0 \leq s \leq t} \{A(s, t) - S(s, t + D)\} > 0\right\} \quad (16)$$

where $b(t)$ and $d(t)$ are the amounts of backlog and delay at time $t \geq 0$ respectively. By applying the Chernoff bound [16] on the right hand side of Equ. 15, we have for $\forall \theta > 0$:

$$P\left\{\max_{0 \leq s \leq t} \{A(s, t) - S(s, t)\} > B\right\} \quad (17)$$

$$\leq e^{-\theta B} E[e^{\theta \max_{0 \leq s \leq t} \{A(s, t) - S(s, t)\}}] \quad (18)$$

$$\leq e^{-\theta B} \sum_{s=0}^t E[e^{\theta A(s, t) - \theta S(s, t)}] \quad (19)$$

$$= e^{-\theta B} \sum_{s=0}^t E[e^{\theta A(0, s) - \theta S(0, s)}] \quad (20)$$

$$\leq e^{-\theta B} \sum_{s=0}^{\infty} M_A(\theta, s) M_S(-\theta, s) \quad (21)$$

consequently, MGF-based stochastic backlog bound is calculated as follows:

$$P(b(t) > B) \leq e^{-\theta B} \sum_{s=0}^{\infty} M_A(\theta, s) M_S(-\theta, s) \quad \forall \theta \in (0, \infty). \quad (22)$$

Similarly, by applying the Chernoff bound [16] on the right hand side of Equ. 16, we have for $\forall \theta > 0$:

$$P\left\{\max_{0 \leq s \leq t} \{A(s, t) - S(s, t + D)\} > 0\right\} \quad (23)$$

$$\leq E[e^{\theta \max_{0 \leq s \leq t} \{A(s, t) - S(s, t + D)\}}] \quad (24)$$

$$\leq \sum_{s=0}^t E[e^{\theta A(s, t) - \theta S(s, t + D)}] \quad (25)$$

$$\leq \sum_{s=D}^{\infty} M_A(\theta, s - D) M_S(-\theta, s) \quad (26)$$

consequently, the MGF-based stochastic delay bound is obtained as follows:

$$P(d(t) > D) \leq \sum_{s=D}^{\infty} M_A(\theta, s - D) M_S(-\theta, s) \quad \forall \theta \in (0, \infty). \quad (27)$$

Acknowledgment

The authors would like to thank Iran Telecommunication Research Center (ITRC) for supporting this research (<http://www.itrc.ac.ir>).

References

- [1] D. Raychaudhuri, X. Jing, I. Seskar, K. Le, J. B. Evans, Cognitive radio technology: From distributed spectrum coordination to adaptive network collaboration, *Pervasive and Mobile Computing* 4 (3) (2008) 278–302.
- [2] I. F. Akyildiz, W.-Y. Lee, M. C. Vuran, S. Mohanty, Next generation/dynamic spectrum access/cognitive radio wireless networks: A survey, *Computer Networks* 50 (13) (2006) 2127–2159.
- [3] O. Akan, O. Karli, O. Ergul, Cognitive radio sensor networks, *IEEE Network* 23 (4) (2009) 34–40.
- [4] A. O. Bicen, O. B. Akan, Reliability and congestion control in cognitive radio sensor networks, *Ad Hoc Networks* 9 (7) (2011) 1154–1164.
- [5] A. O. Bicen, V. C. Gungor, O. B. Akan, Delay-sensitive and multimedia communication in cognitive radio sensor networks, *Ad Hoc Networks* 10 (5) (2012) 816–830.
- [6] A. Slingerland, P. Pawelczak, R. Venkatesha Prasad, A. Lo, R. Hekmat, Performance of transport control protocol over dynamic spectrum access links, in: *2nd IEEE DySPAN 2007*, pp. 486–495.
- [7] Y. Kondareddy, P. Agrawal, Effect of dynamic spectrum access on transport control protocol performance, in: *IEEE GLOBECOM 2009*, pp. 1–6.
- [8] M. Di Felice, K. R. Chowdhury, W. Kim, A. Kassler, L. Bononi, End-to-end protocols for cognitive radio ad hoc networks: An evaluation study, *Performance Evaluation* 68 (9) (2011) 859–875.
- [9] K. Chowdhury, M. Di Felice, I. Akyildiz, TP-CRAHN: a transport protocol for cognitive radio ad-hoc networks, in: *IEEE INFOCOM 2009*, pp. 2482–2490.
- [10] D. Sarkar, H. Narayan, Transport layer protocols for cognitive networks, in: *IEEE INFOCOM 2010*, pp. 1–6.
- [11] T. Issariyakul, L. Pillutla, V. Krishnamurthy, Tuning radio resource in an overlay cognitive radio network for TCP: greed isn’t good, *IEEE Communications Magazine* 47 (7) (2009) 57–63.
- [12] A. K. Al-Ali, K. Chowdhury, TFRC-CR: an equation-based transport protocol for cognitive radio networks, *Ad Hoc Networks* 11 (6) (2013) 1836–1847.
- [13] V. Esmaealzadeh, R. Berangi, S. M. Sebt, E. S. Hosseini, M. Parsinia, CogNS: a simulation framework for cognitive radio networks, *Wireless Personal Communications* 72 (4) (2013) 2849–2865.

- [14] V. Esmaelzadeh, R. Berangi, E. S. Hosseini, O. B. Akan, Modeling of rate-based congestion control schemes in cognitive radio sensor networks, Manuscript submitted for publication.
- [15] V. Esmaelzadeh, R. Berangi, On the optimality of generic rate-based AIMD and AIAD congestion control schemes in cognitive radio sensor networks, *International Journal of Distributed Sensor Networks*, Article ID 614643, in press.
- [16] Y. Jiang, Y. Liu, *Stochastic Network Calculus*, Springer, London, 2008.
- [17] R. L. Cruz, A calculus for network delay, part I: Network elements in isolation, *IEEE Transactions on Information Theory* 37 (1991) 114–131.
- [18] R. L. Cruz, A calculus for network delay, part II: Network analysis, *IEEE Transactions on Information Theory* 37 (1991) 132–141.
- [19] L. Boudec, Thiran, *Network Calculus: A Theory of Deterministic Queuing Systems for the Internet*, Springer, 2001.
- [20] Y. Gao, Y. Jiang, Performance analysis of a cognitive radio network with imperfect spectrum sensing, in: *IEEE INFOCOM 2010 Workshop on Cognitive Wireless Communications and Networking*, 2010, pp. 1–6.
- [21] Y. Gao, J. Yang, X. Zhang, Y. Jiang, Capacity limits for a cognitive radio network under fading channel, in: *Networking 2011 Workshops*, no. 6827 in *Lecture Notes in Computer Science*, Springer Berlin Heidelberg, 2011, pp. 42–51.
- [22] Y. Gao, Y. Jiang, Analysis on the capacity of a cognitive radio network under delay constraints, *IEICE Transactions on Communications E95-B* (4) (2012) 1180–1189.
- [23] T. Xu, X. Chen, X. Xiang, J. Wan, Delay analysis for cognitive radio networks with parallel markov modulated on-off channels, in: *7th International Symposium on Wireless and Pervasive Computing (ISWPC)*, 2012, pp. 1–5.
- [24] Y. Gao, L. Jiang, Y. Jiang, Application of stochastic network calculus in cognitive radio network analysis: A case study, in: *4th IEEE International Conference on Broadband Network and Multimedia Technology (IC-BNMT)*, 2011, pp. 183–187.
- [25] O. B. Akan, On the throughput analysis of rate-based and window-based congestion control schemes, *Computer Networks* 44 (5) (2004) 701–711.
- [26] M. Fidler, An end-to-end probabilistic network calculus with moment generating functions, in: *IEEE 14th International Workshop on Quality of Service (IWQoS)*, 2006, pp. 261–270.

- [27] I. F. Akyildiz, W. Su, Y. Sankarasubramaniam, E. Cayirci, Wireless sensor networks: A survey, *Computer Networks* 38 (4) (2002) 393–422.
- [28] W.-Y. Lee, I. Akyildiz, Optimal spectrum sensing framework for cognitive radio networks, *IEEE Transactions on Wireless Communications* 7 (10) (2008) 3845–3857.
- [29] A. J. D. Rathnayaka, V. M. Potdar, Wireless sensor network transport protocol: A critical review, *Journal of Network and Computer Applications* 36 (1) (2013) 134–146.
- [30] J. Li, P. Mohapatra, Analytical modeling and mitigation techniques for the energy hole problem in sensor networks, *Pervasive and Mobile Computing* 3 (3) (2007) 233–254.
- [31] K. S. Trivedi, *Probability and Statistics with Reliability, Queueing, and Computer Science Applications*, 2nd Edition, Wiley-Interscience, 2001.
- [32] K. Zheng, F. Liu, L. Lei, C. Lin, Y. Jiang, Stochastic performance analysis of a wireless finite-state markov channel, *IEEE Transactions on Wireless Communications* 12 (2) (2013) 782–793.
- [33] C.-S. Chang, Stability, queue length, and delay of deterministic and stochastic queueing networks, *IEEE Transactions on Automatic Control* 39 (5) (1994) 913–931.
- [34] Network simulator version 2, <http://www.isi.edu/nsnam/ns/>.